Optical Materials 52 (2016) 126–133

Contents lists available at ScienceDirect

Optical Materials

journal homepage: www.elsevier.com/locate/optmat

Changes of the local magnetic properties of the optically excited Nd^{3+} ions and their manifestation in the near IR spectra of the $Nd_{0.5}Gd_{0.5}Fe_3(BO_3)_4$ crystal

A.V. Malakhovskii [a,*], S.L. Gnatchenko [b], I.S. Kachur [b], V.G. Piryatinskaya [b], V.L. Temerov [a]

[a] L.V. Kirensky Institute of Physics, Siberian Branch of Russian Academy of Sciences, 660036 Krasnoyarsk, Russian Federation
[b] B. Verkin Institute for Low Temperature Physics and Engineering, National Academy of Sciences of Ukraine, 61103 Kharkov, Ukraine

ARTICLE INFO

Article history:
Received 10 November 2015
Received in revised form 10 December 2015
Accepted 18 December 2015
Available online 22 December 2015

Keywords:
f–f transitions
Nd^{3+} ion
Excited states
Local magnetic properties

ABSTRACT

Polarized absorption spectra of *f–f* transitions $^4I_{9/2} \rightarrow {}^4F_{3/2}$ and $(^2H_{9/2} + {}^4F_{5/2})$ in the Nd^{3+} ion in the $Nd_{0.5}Gd_{0.5}Fe_3(BO_3)_4$ single crystal were studied as a function of temperature in the range of 2–40 K and as a function of magnetic field in the range of 0–65 kOe at 2 K. It was found out that the selection rules for *f–f* electron transitions substantially changed in the magnetically ordered state of the crystal, and they strongly depended on the orientation of the Fe and Nd ions magnetic moments relative to the light polarization. The splitting of the ground and excited states of the Nd^{3+} ion in the exchange field of the Fe sublattice were determined. It was revealed that the value of the exchange splitting (the exchange interaction) in the excited states did not correlate with the theoretical Landé factors. The Landé factors of the excited states were experimentally found. In general, the local magnetic properties in the vicinity of the excited ion depend substantially on its electron state. In particular: (1) in one of the excited states a weak ferromagnetic moment appears, (2) the changes of type of the local magnetic anisotropy take place in some excited states, and (3) in some excited states the energetically favorable orientation of the Nd^{3+} ion magnetic moment is opposite to that in the ground state. In some excited states the nonequivalent Nd^{3+} centers were found out.

1. Introduction

All properties of crystals are totally defined by the electronic structure of ions in the chemical formula of the crystal. The electronically excited ion is similar to the admixture, and, consequently, it changes the local properties of the crystal. A number of phenomena connected with the optical excitation of atoms were observed, e.g., in some rare earth (RE) containing crystals of huntite structure [1–4].

The present work is mainly devoted to study of two phenomena: (1) the influence of the magnetic ordering and magnetic field on the *f–f* electron transitions properties (selection rules, in particular), (2) transformation of the local magnetic and symmetry properties in the excited 4*f* states. Actual problem of the quantum information processing (see e.g., Refs. [5–8]) made the investigations of the local properties of crystals in the optically excited states to be very important. RE containing crystals are widely used in these efforts. So, a change of the local properties near the optically excited atom was used for reading out the information in the quantum memory [6].

Ferroborates of the $RFe_3(BO_3)_4$ type, where R is the RE element, are of the growing interest due to the discovery of the multiferroic properties (i.e. correlation between magnetic, electric and elastic ordering) in many of them [9–13]. The multiferroic effects open the possibility of these materials usage in the new multifunctional devices with the mutual control of magnetic, electric and elastic characteristics. From the viewpoint of the fundamental magnetism, RE ferroborates are of interest due to a wide variety of magnetic properties and phase transitions, which result from the presence of two interacting magnetic subsystems: iron and RE ones [14].

The RE ferroborates have the trigonal huntite-like structure with the space group $R32$ (D_3^7) at high temperatures [15–17]. The unit cell contains three formula units. The RE ions are located at the centers of the trigonal prisms RO_6 (the D_3 symmetry positions). The Fe^{3+} ions are in the C_3 positions inside the octahedrons of oxygen ions. These octahedrons form helicoidal chains along the C_3 axis. With the lowering temperature, some ferroborates undergo a structural phase transition to the $P3_121$ (D_3^4) symmetry phase

* Corresponding author.
E-mail address: malakha@iph.krasn.ru (A.V. Malakhovskii).

http://dx.doi.org/10.1016/j.optmat.2015.12.029
0925-3467/

[17]. It results in the reducing of the RE ion position symmetry to the C_2 one and in appearance of two nonequivalent positions of Fe^{3+} ions (C_2 and C_1).

All RE ferroborates possess antiferromagnetic (AFM) ordering with the Neel temperature in the range of 30–40 K. The AFM ordering is conditioned by the exchange interaction within the iron subsystem [14]. The magnetic ordering of the RE subsystem is induced by the *f–d* exchange interaction with the Fe subsystem. The RE ions, in turn, due to their magnetic anisotropy, usually determine the direction of the Fe^{3+} magnetic moments in the magnetically ordered state. The RE ferroborates can be easy-axis or easy-plane antiferromagnets. In some of them the reorientation phase transitions occur with the temperature change [18,19].

The $Nd_{0.5}Gd_{0.5}Fe_3(BO_3)_4$ crystal, similar to the pure Nd and Gd ferroborates, is multiferroic [20]. Magnetic properties of the crystal $Nd_{0.5}Gd_{0.5}Fe_3(BO_3)_4$ were investigated in Ref. [21]. Below the $T_N = 32$ K the crystal has an easy-plane AFM structure and the spin-reorientation does not occur down to 2 K. At room temperature, the crystal has *R*32 symmetry and the lattice constants: $a = 9.557(7)$ Å and $c = 7.62(1)$ Å [21]. Any structural phase transitions were not found down to 2 K [21]. The distribution of Nd and Gd ions is random that can broaden absorption lines a little. However, this does not affect the subsequent analysis. In the external magnetic field applied in the basal plane of the crystal a hysteresis in magnetization was found at 1–3.5 kOe. The hysteresis was observed at temperatures $T < 11$ K. Additionally the temperature dependence of the magnetic susceptibility had a singularity at $T = 11$ K (when $H < 1$ kOe). These features were ascribed to the appearance of the static magnetic domains at $T < 11$ K. Spectroscopic studies in the external magnetic field $H \perp C_3$ at 2 K [22] also revealed some features indicating the presence of the domains. The Judd–Ofelt spectroscopic parameters of the $Nd_{0.5}Gd_{0.5}Fe_3(BO_3)_4$ single crystal were determined in [23]. Some optical and magneto-optical properties of the crystal were earlier studied in Refs. [22,24].

2. Experimental details

$Nd_{0.5}Gd_{0.5}Fe_3(BO_3)_4$ single crystals were grown from the melt solution on the base of $K_2Mo_3O_{10}$ according to Ref. [3]. The absorption spectra were measured with the light propagating normally to the C_3 axis of the crystal for the light electric vector $\vec{E}$ parallel (the π spectrum) and perpendicular (the σ spectrum) to the C_3 axis and the light propagating along the C_3 axis (the α spectrum). The spectral resolution was approximately equal to 1.5 cm^{-1}. The absorption spectra measured in the σ and α polarizations coincide with each other within the limit of the experimental error. This implies that the absorption mainly occurs through the electric dipole mechanism.

Magnetic field was created by a superconducting solenoid with the Helmholtz type coils. The superconducting solenoid with the sample was placed in the liquid helium and all measurements in the magnetic field were fulfilled at $T = 2$ K. For the temperature measurements of absorption spectra a liquid-helium cooled cryostat was used. It had an internal volume filled by the gaseous helium where the sample was placed.

3. Results and discussion

Absorption spectra of the *f–f* transitions were studied in the temperature range of 2–40 K and in the magnetic field 0–65 kOe at the temperature 2 K. Absorption spectra of the studied *f–f* transitions are given in Fig. 1.

The irreducible representations of states (Table 1) were found from polarizations of the transitions and from the selection rules

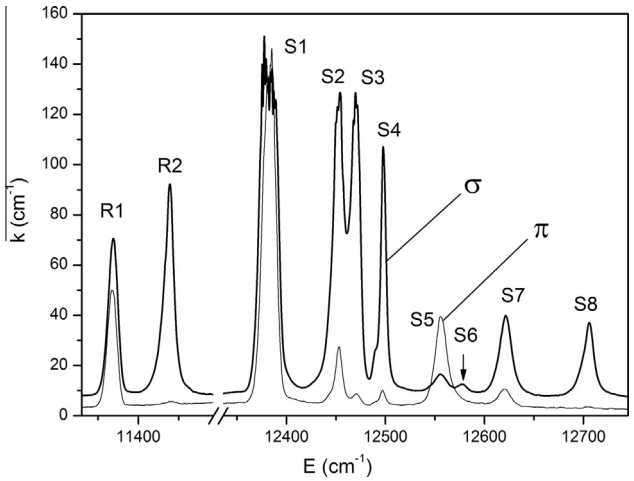

Fig. 1. Polarized absorption spectra of the $^4I_{9/2} \rightarrow {}^4F_{3/2}$ transition (R-band) and of the $^4I_{9/2} \rightarrow {}^2H_{9/2} + {}^4F_{5/2}$ transitions (S-band) at $T = 6$ K.

of Table 2. In crystals there is one more characteristic of states: the crystal quantum number μ. Additionally, in crystals with the axial symmetry, the wave functions of states can be described by $|J, \pm M_J\rangle$ states of the free atom in a first approximation. In a trigonal crystal, for the states with the half integer total moment there are three possible values of the crystal quantum number [25]: $\mu = +1/2, -1/2, 3/2\ (\pm 3/2)$, and between values of μ and M_J there is the correspondence:

$$M_J = \pm 1/2,\ \pm 3/2,\ \pm 5/2,\ \pm 7/2,\ \pm 9/2,\ \pm 11/2,\ \pm 13/2$$
$$\mu = \pm 1/2,\ (\pm 3/2),\ \mp 1/2,\ \pm 1/2,\ (\pm 3/2),\ \mp 1/2,\ \pm 1/2 \qquad (1)$$

The states with $\mu = \pm 1/2$ correspond to the $E_{1/2}$ states and the states with $\mu = (\pm 3/2)$ correspond to the $E_{3/2}$ states in the D_3 group notations. The values of M_J of the studied states (Table 1) were determined in Ref. [26]. In the $|J, \pm M_J\rangle$ function approximation, the effective Landé factor of the Kramers doublet along the C_3 axis is [27]:

$$g_{CM} = 2gM_J. \qquad (2)$$

Here *g* is the Landé factor of the free atom. Values of g_{CM} of the studied states are presented in Table 1. In the same Table the theoretical values of g_C in the $NdFe_3(BO_3)_4$ crystal are given [28]. States with the same μ and different M_J (see Eq. (1)) can mix in crystal, and the resulting g_C can be both smaller and larger than g_{CM}.

In the exchange field of the magnetically ordered iron sublattice, both the ground and the excited states of the Nd^{3+} ion can be split. So, four transitions are possible between components of these splitting. The main possible diagrams of the splitting and transitions are presented in Fig. 2. In Fig. 2A the splitting between *a* and *b* lines is equal to the difference between the exchange splitting of the ground and excited states $\Delta E1$ and $\Delta E2$, respectively: $\Delta E_{12} = (E_a - E_b)$, while in Fig. 2B it is equal to their sum. In both cases, *a* and *b* transitions are supposed to occur without overturn of the magnetic moment. However, then the energetically favorable moment orientation in the excited state of the Fig. 2B diagram will be opposite to that in the ground state. The *c* and *d* transitions in both diagrams occur with the overturn of the magnetic moment, but this does not mean that they are always forbidden (see below). When $\Delta E2 = 0$, the diagrams of Fig. 2A and B are equivalent and transitions *c* and *d* coincide with the transitions *a* and *b*, respectively, and they have no sense separately (Table 3).

Table 1
Parameters of transitions and states. Energies of transitions (E), polarizations and symmetries are given at 40 K. (Details are in the text).

State	Level	E (cm^{-1})	Polar.	Sym.	μ [26]	M_J [26]	g_{CM} [26]	g_C theor. [28]	g_C exper.	$g_\perp$ theor. [28]	$g_\perp$ exper.
$^4F_{3/2}$	R1	11,369	π, σ	$E_{1/2}$	±1/2	±1/2	0.4	0.251	–	0.926	–
	R2	11,436	σ	$E_{3/2}$	3/2	±3/2	1.2	1.562	–	0	–
$^4F_{5/2}$	S1	12,382	π, σ	$E_{1/2}$	±1/2	±1/2	1.03	0.598	–	3.158	–
	S2	12,450	π, σ	$E_{1/2}$	∓1/2	±5/2	5.14	4.713	~3.7	0.096	~0
	S3	12,467	σ	$E_{3/2}$	3/2	±3/2	3.09	2.576	–	0	–
$^2H_{9/2}$	S4	12,495	π, σ	$E_{1/2}$	±1/2	±7/2	6.36	4.633	3.68	1.989	1.64
	S5	12,553	π, σ	$E_{1/2}$	±1/2	±1/2	0.909	0.982	0	3.995	4.0
	S6	12,578	σ	$E_{3/2}$	3/2	±3/2	2.73	2.169	0	0	0
	S7	12,620	π, σ	$E_{1/2}$	∓1/2	±5/2	4.55	2.765	0	2.877	3.47
	S8	12,702	σ	$E_{3/2}$	3/2	±9/2	8.18	7.788	8.0	0	0

Table 2
Selection rules for electric dipole transitions in the D_3 symmetry.

	$E_{1/2}$	$E_{3/2}$
$E_{1/2}$	π, $\sigma(\alpha)$	$\sigma(\alpha)$
$E_{3/2}$	$\sigma(\alpha)$	π

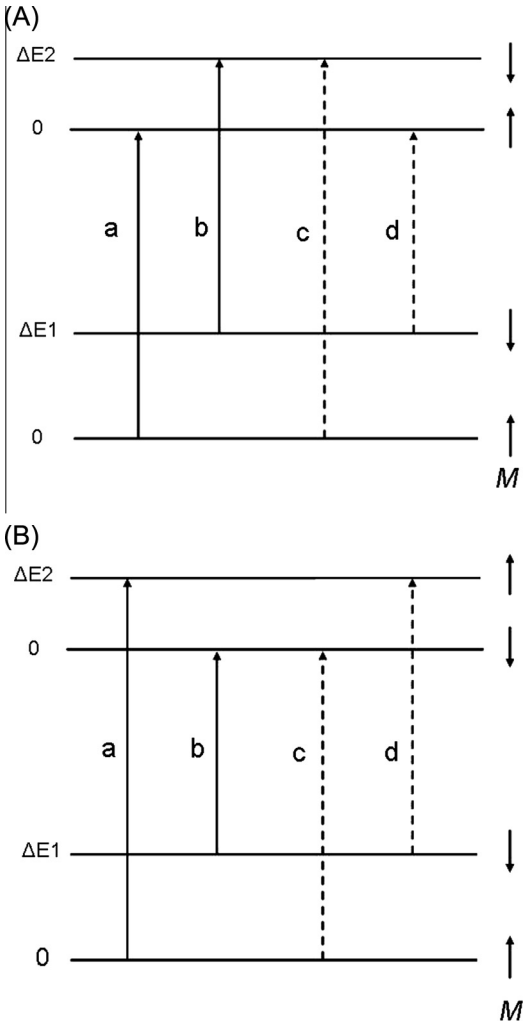

Fig. 2. (A and B) Diagrams of transitions in the magnetically ordered state in the zero magnetic field.

3.1. Temperature behavior of transitions into the $E_{3/2}$ states

The characteristic feature of the $E_{3/2}$ states is that $g_\perp = 0$ in these states (see Table 3). As far as magnetic moments of the iron ions are in the plane perpendicular to the C_3 axis, the Nd^{3+} states with $g_\perp = 0$ should not split in the exchange field. Only two of the absorption lines, corresponding to the transitions into the $E_{3/2}$ states, revealed a temperature dependent splitting below the T_N (Fig. 3). So, this splitting should be equal to the splitting of the Nd^{3+} ground state $\Delta E1$. We supposed the exchange splitting of the ground state at 6 K to be average of values 10 and 8.8 cm^{-1} (see Fig. 3), i.e., 9.4 cm^{-1}, that corresponds to H_{ex} = 84.4 kOe, taking into account the theoretical value $g_\perp = 2.385$ in the ground state of $NdFe_3(BO_3)_4$ [28]. The exchange splitting of the Nd^{3+} ion ground state found in $NdFe_3(BO_3)_4$ was 8.8 cm^{-1} [28].

The different values of the exchange splitting found from the different transitions mean that the electron transition has an influence on the local properties of the crystal not only in the excited but also in the ground state. Indeed, electron transitions occur due to the mixing of the initial and final states by the time dependent perturbation caused by the electromagnetic wave. Similar phenomenon was earlier noted also in Ref. [27]. The singularities in the temperature dependences of Fig. 3 in the region of 14–16 K indicate that there are some local distortions in the corresponding excited states. Not all transitions demonstrate the temperature dependent splitting ΔE_{12} connected with the exchange splitting of the ground state (Table 3). This means that the transition "*b*" from the upper sublevel of the ground state exchange splitting is forbidden.

3.2. $^4I_{9/2} \rightarrow {}^4F_{3/2}$ transition (R band)

The geometry of measurements in the magnetic field is presented in Fig. 4. The behavior of the R1a line energy and intensity in the magnetic field $H \perp C_3$ is shown in Fig. 5. There was an unexpected observation that the energy of transition depended on the polarization. In particular, this occurs in the region of 0–4 kOe in the many domain state of the crystal, and at $H_\perp > 4$ kOe (one domain state). This looks like the splitting of the states in the crystal field that is not possible for the Kramers doublets. Such phenomena can be accounted for by the absorption of the Nd^{3+} ion in two nonequivalent positions. In the former case these can be domains and domain walls and in the latter case: equivalent inverse twins, on the one hand, and the boundaries between the twins, on the other hand. The magnetic field increases and reveals this nonequivalence. The same phenomena were earlier observed at the transition $^4I_{9/2} \rightarrow {}^4G_{5/2} + {}^2G_{7/2}$ in the same crystal [22]. The resembling phenomenon was observed in $ErAl_3(BO_3)_4$ and $ErFe_3(BO_3)_4$ crystals [29]. In the $ErAl_3(BO_3)_4$ the local symmetry of Er^{3+} ($^4I_{15/2}$) ion is D_3, the same as in the studied crystal. A small splitting (0.11 cm^{-1}) of one of the absorption lines was observed without the external magnetic field. In the $ErFe_3(BO_3)_4$ (with the lower symmetry) the same splitting was much larger (11.3 cm^{-1}).

In the R1 state $g_\perp \neq 0$ (Table 3) and the exchange splitting is possible. However, no splitting of the R1 line was observed both

Table 3
Polarizations of transitions in the paramagnetic state ($T > T_N$) and of transitions (a, b, c, d) between components of the ground and excite states exchange splitting at $H = 0$, diagrams describing these transitions, the theoretical Landé factor of the Nd^{3+} ion in the basal plane in the $NdFe_3(BO_3)_4$ crystal ($g_\perp$), exchange splitting of the excited states ($\Delta E2$), temperature dependent exchange splitting of absorption lines at 6 K ($\Delta E_{12} = E_a - E_b = \Delta E1 \pm \Delta E2$), the energetically favorable moment orientations in the excited states relative to that in the ground state in the zero magnetic field ($M2$).

Transitions	$T > T_N$	a	b	c	d	Diagram	$g_\perp$ theor. [28]	$\Delta E2$	ΔE_{12}	$M2$
R1 ($\rightarrow E_{1/2}$)	π, σ	π, σ	0	–	–	2A, 2B	0.926	–	–	
R2 ($\rightarrow E_{3/2}$)	σ	σ	σ	–	–	2A, 2B	0	0	10.0	
S2 ($\rightarrow E_{1/2}$)	π, σ	π, σ	π, ?	π, ?	0	2A	0.096	2.7	9.6	(+)
S4 ($\rightarrow E_{1/2}$)	π, σ	π, σ	π, σ	–	–	2A, 2B	1.989	0	8.0, 9.0	
S5 ($\rightarrow E_{1/2}$)	π, σ	π, σ	0	–	–	2A, 2B	3.995	0	–	
S6 ($\rightarrow E_{3/2}$)	σ	σ	0	–	–	2A, 2B	0	0	–	
S7 ($\rightarrow E_{1/2}$)	π, σ	π, σ	0	–	–	2A, 2B	2.877	0	–	
S8 ($\rightarrow E_{3/2}$)	σ	σ	σ	–	–	2A, 2B	0	0	8.8	
D1 ($\rightarrow E_{1/2}$)	π, σ	π, σ	0	$M \| \sigma$	NCD	2A	0.043	7	–	(−)
D2 ($\rightarrow E_{1/2}$)	π, σ	π	π	σ	0	2B	1.385	2	14	(+)
D3 ($\rightarrow E_{3/2}$)	σ	σ	0	–	–	2A, 2B	0	0	–	
D4 ($\rightarrow E_{1/2}$)	π, σ	π, σ	0	σ	0	2A	2.617	12	–	(+?)
D5 ($\rightarrow E_{1/2}$)	π, σ	π, σ	π	$M \| \pi$	0	2B	0.755	7.5	~17	(+?)
D6 ($\rightarrow E_{1/2}$)	π, σ	π	0	σ	0	2B	1.538	0.4	–	(−)
D7 ($\rightarrow E_{3/2}$)	σ	σ	0	–	–	2A, 2B	0	0	–	

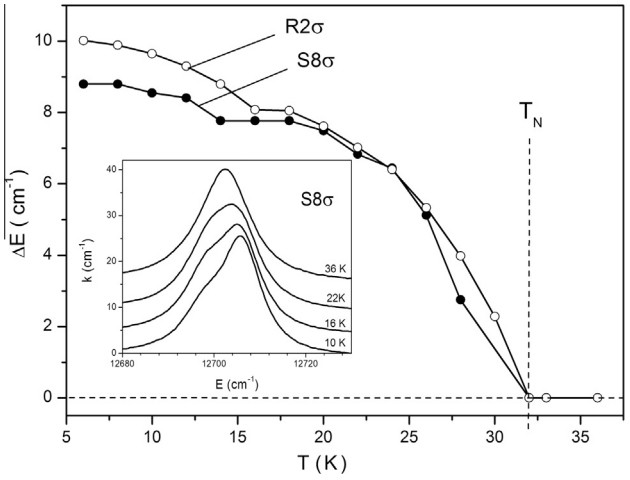

Fig. 3. Temperature dependences of the exchange splitting of transitions into the states of the $E_{3/2}$ symmetry. Inset: transformation of the S8σ spectrum with the temperature.

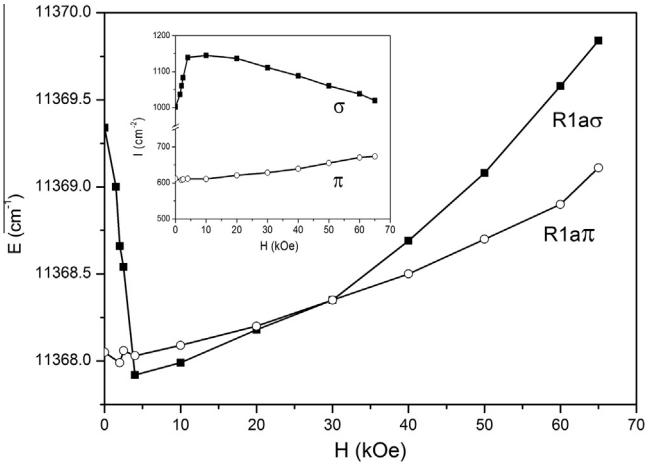

Fig. 5. Energies of the R1a line in two polarizations as a function of the magnetic field $H \perp C_3$. Inset: intensities of the same lines.

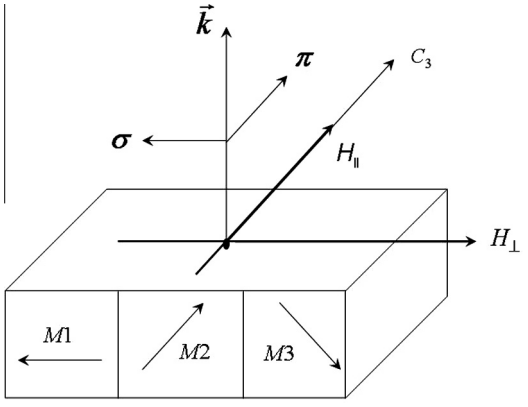

Fig. 4. Geometry of measurements. M1, M2 and M3 are three types of domains in the basal plane.

at 2 K (in one domain state at $H_\perp = 4$ kOe) and at temperatures between 2 K and the Neel temperature. For the Fig. 2A diagram, the lack of the R1 line splitting at $H_\perp = 4$ kOe ($T = 2$ K) and as a function of temperature is possible in several cases. (1) The exchange splitting of the excited and ground states are equal and R1c and R1d transitions are forbidden. (2) The exchange splitting of the excited state is equal to zero and the equivalent R1b and R1d transitions are forbidden. (3) Only the R1a transition is allowed. The latter variant is preferable. For the Fig. 2B diagram only the third variant is possible.

$H = 4$ kOe is also the field of the spin-flop [21], i.e., magnetic moments of all ions become perpendicular to the magnetic field. Then Fig. 5 inset testifies that the σ absorption for the R1a transition is more probable, when magnetic moments of the Nd^{3+} ions in the ground state are perpendicular to the σ-polarization (Fig. 4). The π-polarization is always perpendicular to the magnetic moments.

The splitting of the R2 line both in $H \perp C_3$ and $H \| C_3$ was not observed. For $H \perp C_3$ it is natural since $g_\perp = 0$ in the excited state (Table 3). In this case the diagrams of Fig. 2A and B are equivalent (Table 3). The temperature dependent splitting of the R2 line was presented above (Fig. 3).

3.3. $^4I_{9/2} \rightarrow {}^2H_{9/2} + {}^4F_{5/2}$ transitions (S band)

3.3.1. S2 line

This line can be studied only in the π-polarization because of the high intensity of the S2σ line (see Fig. 1). Since the experiments in magnetic field were fulfilled at $T = 2$ K, only transitions from the lowest level of the ground state, S2a and S2c in the diagram of

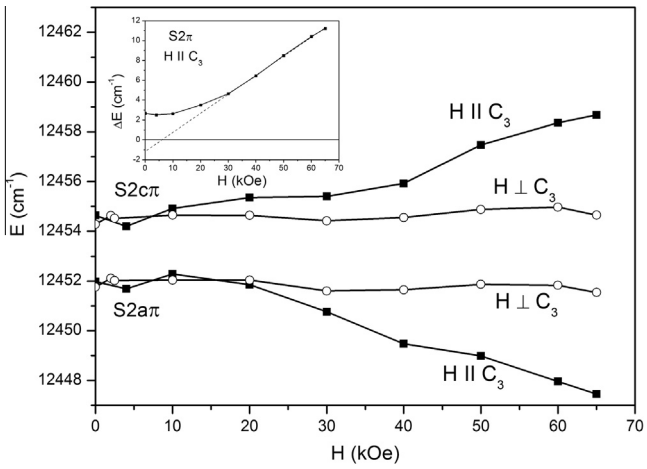

Fig. 6. Energies of the S2aπ and S2cπ transitions as a function of the magnetic field $H \perp C_3$ and $H \| C_3$. Inset: Splitting of the S2 line $\Delta E_{12} = E_a - E_b$ in the magnetic field $H \| C_3$.

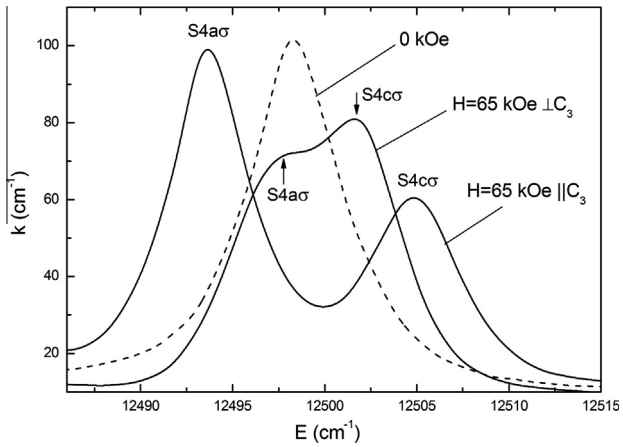

Fig. 7A. Absorption spectra of the S4σ transition in the magnetic fields $H \perp C_3$ and $H \| C_3$.

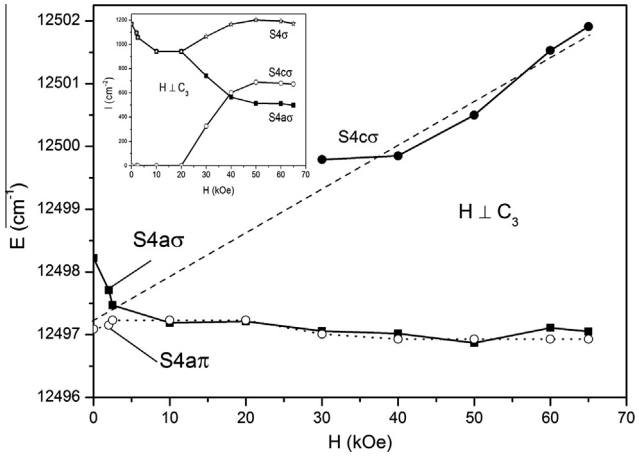

Fig. 7B. Energies of the S4aπ, S4aσ and S4cσ transitions as a function of the magnetic field $H \perp C_3$. Inset: field dependences of intensities of the S4σ transitions.

Fig. 2A, were observed. The splitting between them gives the exchange splitting of the excited state $\Delta E2 = 2.7\ cm^{-1}$ (Fig. 6, Table 3). In the field $H \perp C_3$ the energies of the S2aπ and S2cπ transitions change slightly and identically, but in the field $H \| C_3$ the splitting increases (Fig. 6). This behavior is apparently due to the strong magnetic anisotropy in the S2 state. In particular, as opposed to the ground state, the C_3 direction is the easy axis for the Nd^{3+} ion magnetic moment in the S2 state. Indeed, $g_C \gg g_\perp$ in this state (Table 1). If the magnetic field is applied along the easy direction, then the magnetic moments of the antiferromagnet orientate perpendicular to the magnetic field. In this case the splitting of the S2 doublet in the magnetic field (Fig. 6, inset) should be described by the formula:

$$\Delta E = \mu_B g_M \left(H_{Fe}^2 + H^2\right)^{1/2} \quad (3)$$

under the assumption that orientation of the Fe magnetic moments remains purely antiferromagnetic. H_{Fe} in (3) is the exchange field Fe–Nd and g_M is the Landé factor of the Nd^{3+} ion in the direction of its magnetic moment in the excited state. At the large magnetic field H the formula (3) transforms into the straight line going through the origin of coordinates. However in reality it is not so (see Fig. 6, inset). The dependence of the Fig. 6, inset can be obtained if we substitute H for $H + \Delta H$, where ΔH = constant. This value ΔH corresponds to some exchange field and to some spontaneous magnetic moment along the external magnetic field.

A temperature dependent splitting of the S2π line is also observed [24]. At $T = 6$ K it is $9.6\ cm^{-1}$ (Table 3). This is just between two values of the ground state exchange splitting mentioned above. However, because of the small exchange splitting of the excited state it is impossible to differentiate S2aπ and S2cπ lines and S2bπ and S2dπ lines (Fig. 2A) during decomposition of the S2 line spectrum. Additionally, as mentioned above, the obtained value of the ground state exchange splitting depends on the transition from which it is found.

3.3.2. S4 line

Fig. 7A demonstrates transformation of the σ-polarized S4 line spectrum in the magnetic fields $H \perp C_3$ and $H \| C_3$. The behavior of the S4 lines positions in the field $H \perp C_3$ is shown in Fig. 7B. In the one domain state of the crystal ($H_\perp > 4$ kOe) the energies of the S4aσ and S4aπ lines are equal (Fig. 7B). Difference of these energies at $H_\perp < 4$ kOe, as mentioned above, can be connected with the absorption in domains and domain walls. At $H_\perp > 20$ kOe the σ-polarized line S4cσ appears, but S4cπ line does not appear (Fig. 7B and B, inset). The asymmetric changes of the S4aσ and S4cσ transitions energies as a function of the magnetic field $H \perp C_3$ (Fig. 7B) is probably connected with the change of the ground state energy. Extrapolation of the field dependence of the S4cσ line energy to $H = 0$ (Fig. 7B) permits us to suppose that the exchange splitting $\Delta E2$ of the S4 state is close to zero.

The behavior of the S4 lines positions in the field $H \| C_3$ is presented in Fig. 7C. At this field orientation the S4c line appears in both polarizations already at ~10 kOe. The magnetic field $H \| C_3$ does not create the one domain state. Therefore, a small splitting observed in the weak field is apparently connected only with the domain structure (Fig. 7C). It is rather surprising that in one domain state at the low magnetic field there is no exchange splitting of the excited state, since according to the theory $g_\perp \neq 0$ in this state (Table 3). This means that there is no Fe–Nd exchange interaction in the considered excited state of the Nd^{3+} ion. Consequently, the diagrams of Fig. 2A and B are equivalent. The observed splitting $11.15\ cm^{-1}$ in the field $H_\| = 65$ kOe is actually the splitting of the paramagnetic ion. Corresponding $g_C = 3.68$ is of the same order of magnitude as the theoretical values of g_C and g_{CM} (Table 1). The splitting $4.97\ cm^{-1}$ in the field $H_\perp = 65$ kOe corresponds to $g_\perp = 1.64$ that is close to the theoretical value in the $NdFe_3(BO_3)_4$ crystal (Table 1).

The temperature dependent splitting of the S4 line both in the π and σ polarizations is also observed. The splitting values at 6 K are

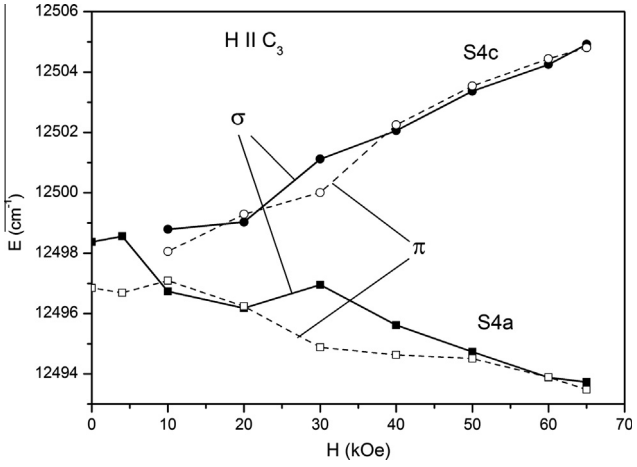

Fig. 7C. Energies of the S4 transitions as a function of magnetic field $H||C_3$.

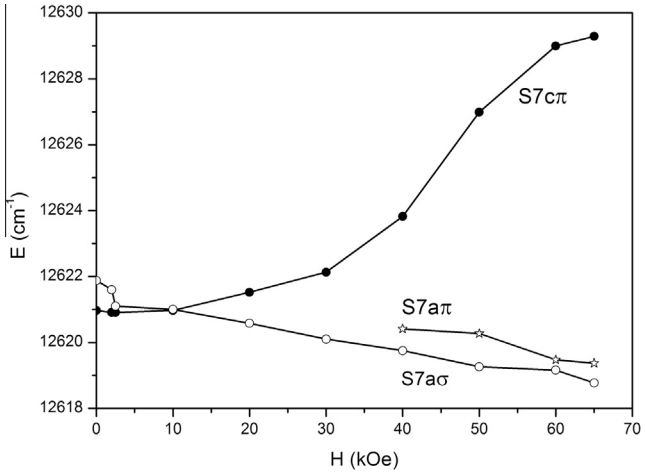

Fig. 9. Energies of the S7 transitions as a function of the magnetic field $H \perp C_3$.

8.0 and 9.0 cm^{-1}, respectively (Table 3). They are a little different, since the experiment is made in the zero magnetic field, i.e., in the many domain state (see Fig. 7B). They are also close to the found above exchange splitting of the ground state, because the exchange splitting of the S4 excited state in the magnetically homogeneous state of the crystal is found to be zero.

3.3.3. S5 and S6 lines

Positions of S5 lines as a function of the magnetic field are presented in Fig. 8. The S5 line is not split at $H = 0$, i.e., there is no exchange splitting in spite of $g_\perp \neq 0$ in the S5 state (Table 3), and the Nd^{3+} ion is actually in the paramagnetic state. The observed splitting in the external magnetic field $H \perp C_3$ (Fig. 8) corresponds to $g_\perp = 4.0$. This value is very close to the theoretical $g_\perp$ in $NdFe_3(BO_3)_4$ crystal (Table 3). The zero splitting of the S5 line in the magnetic field $H||C_3$ (Fig. 8) indicates that there is a strong local one-ion magnetic anisotropy of the easy plane type in the S5 state.

The S6 line does not reveal a splitting both in $H \perp C_3$ and in $H||C_3$. It is quite natural that the S6 line is not split in the exchange field and in the external field $H \perp C_3$ since theoretically $g_\perp = 0$ in the S6 state (Table 3). However, in $H||C_3$ the S6 line could split in the external field. The absence of the splitting can be caused by the forbiddenness of the transition into the second component of the excited state exchange splitting. The temperature dependent splitting of the S5 and S6 lines is not observed, i.e., transitions from the upper sublevel of the ground state exchange splitting are forbidden (Table 3).

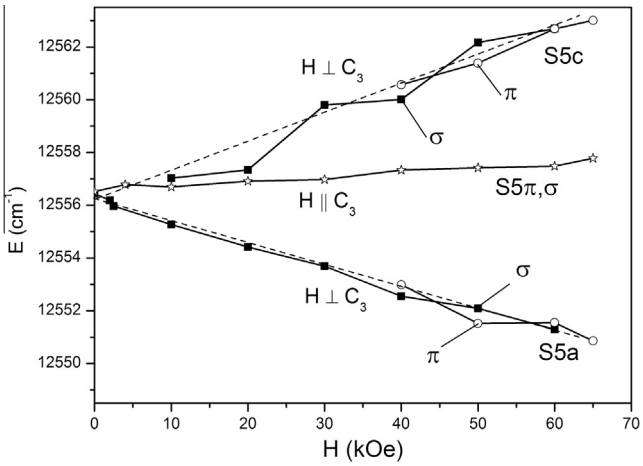

Fig. 8. Energies of the S5 transitions as a function of the magnetic field $H \perp C_3$ and $H||C_3$.

3.3.4. S7 line

In the one domain state ($H = 4$ kOe) the S7 line is not split by the exchange field (Fig. 9, Table 3). Consequently, Nd^{3+} ion in the S7 excited state is in the paramagnetic state, in spite of the non zero theoretical $g_\perp$ in the D_3 symmetry (Table 3). The splitting in the magnetic field $H \perp C_3$ is observed only in the π-polarization and between π and σ-polarizations (Fig. 9), i.e., S7cσ transition is forbidden in the magnetic field $H \perp C_3$ ($M \perp \sigma$). The splitting in the field $H_\perp = 65$ kOe corresponds to $g_\perp = 3.47$ that is close to the theoretical value in $NdFe_3(BO_3)_4$ (Table 1). The non linear splitting as a function of $H_\perp$ (Fig. 9) is, probably, due to the anisotropy in the basal plane.

In the magnetic field $H||C_3$ the splitting of the S7 line is not observed in spite of the theoretical $g_C \neq 0$ in the S7 state (Table 1) that indicates to the strong easy plane anisotropy. The temperature dependent splitting of the S7 line is also not observed and, consequently, the S7b line is forbidden (Table 3).

3.3.5. S8 line

This line exists only in the σ-polarization (Fig. 1). Its energy behavior in the fields $H \perp C_3$ and $H||C_3$ is presented in Fig. 10. The exchange splitting ($H = 0$) is not observed in accordance with the theoretical $g_\perp = 0$ in the S8 state (Table 3), and, consequently, the Nd^{3+} ion is in the paramagnetic state. The splitting 24.3 cm^{-1} in the field $H_{||} = 65$ kOe (Fig. 10) corresponds to $g_C = 8.0$ that is close to the theoretical values of g_C and g_{CM} (Table 1). The behavior of the S8 line in the fields $H \perp C_3$ and $H||C_3$ (Fig. 10) is opposite to that of the S5 line (Fig. 8). In particular, these dependences testify that the magnetic anisotropy of the Nd^{3+} ion in the S8 state is of the easy axis type while in the S5 state it is of the easy plane type. Anisotropy in the S8 state agrees with the theoretical values of the Landé factor, while in the S5 state it deviates from the theory. The temperature dependent splitting of the S8σ line was shown in Fig. 3.

In conclusion it is necessary to generalize some observed regularities. To give a complete picture we added in Table 3 the results obtained earlier [22] for the transition $^4I_{9/2} \rightarrow {}^4G_{5/2} + {}^2G_{7/2}$ (D-band) and added Fig. 11, related to the same transition.

Fig. 5, inset and Fig. 11 demonstrate substantial dependence of the transitions intensities on the orientation of the Fe and Nd magnetic moments. Especially this refers to the D1cσ line (Fig. 11) whose intensity goes to zero at the spin flop field, when magnetic moments of Fe and Nd ions in the ground state become

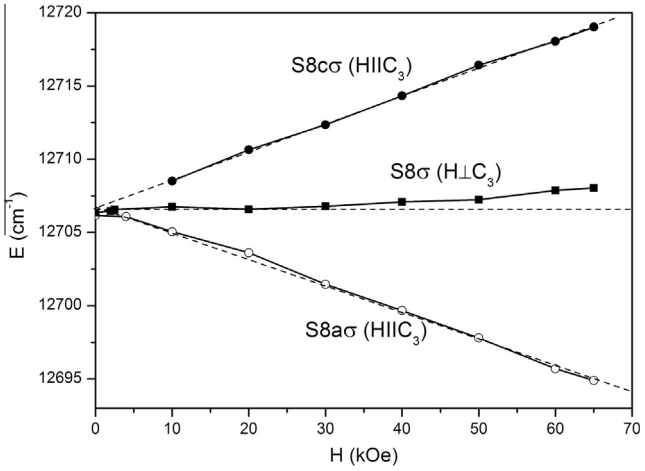

Fig. 10. Energies of the S8 transitions as a function of the magnetic field $H \perp C_3$ and $H||C_3$.

perpendicular to the σ-polarization. The intensities of the R1aσ (Fig. 5, inset), D2cσ and D4aσ (Fig. 11) lines, on the contrary, increase at the same conditions. However, excited states of all discussed transitions have identical symmetry $E_{1/2}$ in the paramagnetic state of the crystal. Apparently, the intensities of the transitions depend mainly on the Nd magnetic moment orientation, since they change also in the fields $H > 4$ kOe, when orientation of the Fe magnetic moment practically does not change (Fig. 11).

Only polarizations of "*a*" and "*b*" components of S4 and S8 transitions coincide with those in paramagnetic state of the crystal, but the majority of components of all transitions are forbidden at all (Table 3). However, at the possible decrease of the local symmetry with the magnetic ordering, all transitions should be allowed at all polarizations. Above observations show, that, first, the selection rules by magnetic moment acquire the great importance and, secondly, the local symmetry is different in different excited states and is unknown.

For the $NdFe_3(BO_3)_4$ crystal in Ref. [30] there were suggested the following Hamiltonians of Nd and Fe ions from the *i*th sublattice ($i = 1, 2$) in the presence of magnetic field:

$$\widehat{H}_i\ (\mathrm{Nd}) = \widehat{H}^i_{CF} - g_J \mu_B \overrightarrow{J}_i \cdot (\overrightarrow{H} + \lambda_{fd}\overrightarrow{M}_i), \tag{4}$$

$$\widehat{H}_i\ (\mathrm{Fe}) = -g_S \mu_B \overrightarrow{S}_i \cdot (\overrightarrow{H} + \lambda \overrightarrow{M}_j + \lambda_{fd}\vec{m}_i). \tag{5}$$

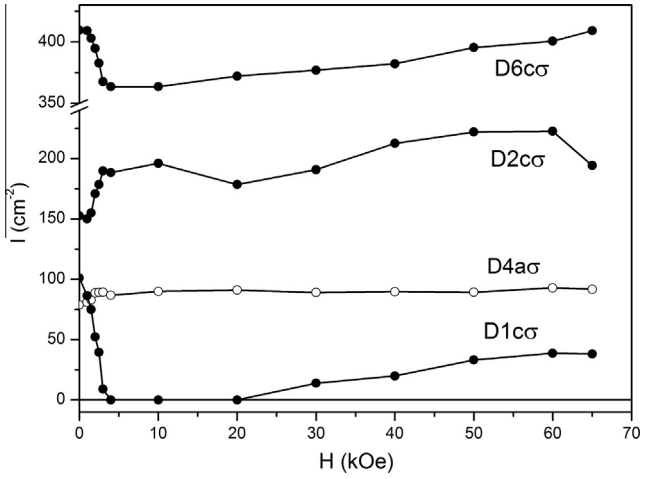

Fig. 11. Intensities of transitions as a function of magnetic field $H \perp C_3$.

Here $\widehat{H}^i_{CF}$ is the crystal field Hamiltonian, whose form is determined by the symmetry of the local environment of an Nd ion in the ground state, g_J is the Landé factor and $\widehat{J}_i$ is the operator of the angular momentum of the Nd ion, $g_S = 2$ is the Landé factor and $\overrightarrow{S}_i$ is the operator of the spin moment of an iron atom, $\lambda_{fd} < 0$ and $\lambda < 0$ are the molecular constants of the AFM interactions Nd–Fe and Fe–Fe, respectively, $\vec{M}_i$ and $\vec{m}_i$ are the magnetic moments of the Fe and Nd ions, respectively. Hamiltonians (4) and (5) are written, taking into account that according to Ref. [18] RE ions in ferroborates do not interact with iron ions positioned in the same crystal plane, but reveal the AFM interaction with the iron ions in the adjacent planes. Interaction inside the RE subsystem is not taken into account since it is negligibly small. Parameters of the CF in $NdFe_3(BO_3)_4$ were determined, basing on its absorption spectra [28]. These parameters permitted to find the Landé factors of Nd ion and to describe the magnetic properties of the $NdFe_3(BO_3)_4$ crystal [28,30]. Crystal structure of the $Nd_{0.5}Gd_{0.5}Fe_3(BO_3)_4$ is identical to that of the $NdFe_3(BO_3)_4$, and the absorption spectra of these crystals are very close. Therefore we used the Landé factors obtained in Ref. [28] as a first approximation (Table 1 and 3). In some cases they were close to the experimentally found ones, but there were also substantial discrepancies, in particular, in the S5, S6 and S7 states (Tables 1 and 3). Consequently, the local magnetic anisotropy of the Nd^{3+} ion in these states substantially differs from the predicted ones. This indicates to the deviation of the local CF in the excited states of the Nd ion from that in the ground state. Possibility of the photoinduced single-ion magnetic anisotropy was theoretically considered, e. g., in Ref. [31]. The exchange interactions in (4) and (5) remain to be the parameters found experimentally.

The exchange field of the Fe sublattice is directed perpendicular to the C_3 axis. Therefore, the exchange splitting of the excited Nd^{3+} states with $g_\perp = 0$ should be zero. It is really so (see Table 3). However, in some excited states the Nd^{3+} ions revealed the zero exchange splitting, i. e., the zero exchange interaction with the Fe sublattice, in spite of the not zero Landé factor $g_\perp$ (Table 3). Thus, the value of the exchange splitting (the exchange interaction) does not correlate with the theoretical Landé factor $g_\perp$ of the Nd^{3+} ion (Table 3). It is necessary to note that the Hamiltonian (4) does not take into account the anisotropic and antisymmetric exchange, which can be one of the reasons of the peculiar magnetic properties of the Nd ion in the excited states. In particular, the antisymmetric exchange provides the mutually perpendicular orientation of the magnetic moments of the Fe and Nd ions.

In general, the local magnetic properties in the vicinity of the excited ion substantially depend on its electron state. From the above consideration it is clear that this is connected with the change of the local interaction of the excited ion with the environment. Thus, the knowledge of the crystal field in the ground state cannot provide the theoretical prediction of the local magnetic and other properties in the excited states.

4. Summary

Polarized absorption spectra of *f*–*f* transitions $^4I_{9/2} \rightarrow {}^4F_{3/2}$ and $(^2H_{9/2} + {}^4F_{5/2})$ in the Nd^{3+} ion in the $Nd_{0.5}Gd_{0.5}Fe_3(BO_3)_4$ single crystal were studied as a function of temperature in the range of 2–40 K and as a function of magnetic field in the range of 0–65 kOe at 2 K. In the magnetically ordered state of the crystal, the splitting of the ground and excited states of the Nd^{3+} ion in the exchange field of the Fe sublattice were determined. It was found out that the value of the Nd^{3+} ion states exchange splitting (the exchange interaction) did not correlate with the theoretical Landé factor $g_\perp$ of the states (Table 3). The Landé factors of the excited states were experimentally found. In some states they

substantially differ from the theoretically predicted ones. This testifies to the deviation of the local CF in the excited states of the Nd ion from that in the ground state. In general, the local magnetic properties in the vicinity of the excited ion substantially depend on its electron state. In particular: (1) in one of the excited states a weak ferromagnetic moment appears in magnetic field, (2) the changes of type of the local magnetic anisotropy take place, and (3) in some excited states (see Table 3) the energetically favorable orientation of the Nd^{3+} ion magnetic moment is opposite to that in the ground state.

Energies of some transitions depend on their polarization. Such phenomenon can be accounted for by the absorption of the Nd^{3+} ions in two nonequivalent positions. In the many domain state ($H_{\perp} < 4$ kOe) they can be domains and domain walls. In the one domain state ($H_{\perp} > 4$ kOe) they can be equivalent inverse twins, on the one hand, and the boundaries between the twins, on the other hand. The magnetic field increases and reveals this nonequivalence. This phenomenon is observed only in some excited states. Consequently, it is connected with the electron state dependent local distortions.

It was found out that the selection rules for the electron transitions substantially changed in the magnetically ordered state of the crystal. They are different for the different transitions with the same symmetry in the paramagnetic state of the crystal (Table 3), and they strongly depend on the orientation of the Nd and Fe ions magnetic moments relative to the light polarization. Some transitions appear only in the magnetic field. It is also worth noting that the majority of the studied excited states has identical symmetry $E_{1/2}$ in the paramagnetic state of the crystal, but they have a great variety of the local magnetic properties. There can be two sources of these features. First, these states refer to different multiplets and (or) have different M_J in the $|J, \pm M_J\rangle$ representation (Table 1). Second, in spite of the axial crystal symmetry, the magnetic moments in the ground state are in the plane perpendicular to the C_3 axis. Therefore, they create one more quantization axis besides the C_3 one, and, consequently, they create the peculiar selection rules for the electron transitions, which depend also on the excited states because the electronically excited atom modifies the local symmetry and magnetic properties of the crystal.

Acknowledgements

The work was supported by the Russian Foundation for Basic Researches Grant 16-02-00273 and by the President of Russia Grant No. Nsh-2886.2014.2.

References

[1] A.V. Malakhovskii, A.L. Sukhachev, S.L. Gnatchenko, I.S. Kachur, V.G. Piryatinskaya, V.L. Temerov, A.S. Krylov, I.S. Edelman, J. Alloys Comp. 476 (2009) 64.
[2] A.V. Malakhovskii, S.L. Gnatchenko, I.S. Kachur, V.G. Piryatinskaya, A.L. Sukhachev, V.L. Temerov, Eur. Phys. J. B 80 (2011) 1.
[3] A.V. Malakhovskii, S.L. Gnatchenko, I.S. Kachur, V.G. Piryatinskaya, A.L. Sukhachev, I.A. Gudim, J. Alloys Compd. 542 (2012) 157.
[4] A.V. Malakhovskii, S.L. Gnatchenko, I.S. Kachur, V.G. Piryatinskaya, A.L. Sukhachev, A.E. Sokolov, A.Ya. Strokova, A.V. Kartashev, V.L. Temerov, Crystallogr. Rep. 58 (2013) 135.
[5] J.J. Longdell, M.J. Sellars, Phys. Rev. A 69 (2004) 032307.
[6] J.H. Wesenberg, K. Mølmer, L. Rippe, S. Kröll, Phys. Rev. A 75 (2007) 012304.
[7] A.V. Kimel, A. Kirilyuk, T. Rasing, Laser Photon. Rev. 1 (2007) 275.
[8] A.I. Lvovsky, B.C. Sanders, W. Tittel, Nat. Photon. 3 (2009) 706.
[9] A.K. Zvezdin, S.S. Krotov, A.M. Kadomtseva, G.P. Vorob'ev, Yu.F. Popov, A.P. Pyatakov, L.N. Bezmaternykh, E.A. Popova, Pis'ma v ZhETF 81 (2005) 335 [JETP Lett. 81 (2005) 272].
[10] A.K. Zvezdin, G.P. Vorob'ev, A.M. Kadomtseva, Yu.F. Popov, A.P. Pyatakov, L.N. Bezmaternykh, A.V. Kuvardin, E.A. Popova, Pis'ma v ZhETF 83 (2006) 600 [JETP Lett. 83 (2006) 509].
[11] F. Yen, B. Lorenz, Y.Y. Sun, C.W. Chu, L.N. Bezmaternykh, A.N. Vasiliev, Phys. Rev. B 73 (2006) 054435.
[12] R.P. Chaudhury, F. Yen, B. Lorenz, Y.Y. Sun, L.N. Bezmaternykh, V.L. Temerov, C. W. Chu, Phys. Rev. B 80 (2009) 104424.
[13] A.M. Kadomtseva, Yu.F. Popov, G.P. Vorob'ev, A.P. Pyatakov, S.S. Krotov, P.I. Kamilov, V.Yu. Ivanov, A.A. Mukhin, A.K. Zvezdin, L.N. Bezmaternykh, I.A. Gudim, V.L. Temerov, Fiz. Nizk. Temp. 36 (2010) 640 [Low Temp. Phys. 36 (2010) 511].
[14] A.N. Vasiliev, E.A. Popova, Fiz. Nizk. Temp. 32 (2006) 968 [Low Temp. Phys. 32 (2006) 735].
[15] J.C. Joubert, W. White, R. Roy, J. Appl. Cryst. 1 (1968) 318.
[16] J.A. Campá, C. Cascales, E. Gutiérrez-Puebla, M.A. Monge, I. Rasines, C. Ruíz-Valero, Chem. Mater. 9 (1997) 237.
[17] S.A. Klimin, D. Fausti, A. Meetsma, L.N. Bezmaternykh, P.H.M. van Loosdrecht, T.T.M. Palstra, Acta Crystallogr. B 61 (2005) 481.
[18] A.I. Pankrats, G.A. Petrakovsky, L.N. Bezmaternykh, O.A. Bayukov, ZhETF 126 (2004) 887 [JETP 99 (2004) 766].
[19] C. Ritter, A. Vorotynov, A. Pankrats, G. Petrakovskii, V. Temerov, I. Gudim, R. Szymczak, J. Phys.: Condens. Matter 20 (2008) 365209.
[20] A.M. Kadomtseva, Yu.F. Popov, G.P. Vorob'ev, A.A. Mukhin, V.Yu. Ivanov, A.M. Kuz'menko, A.S. Prokhorov, L.N. Bezmaternykh, V.L. Temerov, I.A. Gudim, in: Proceedings of the XXI International Conference "New in Magnetism and Magnetic Materials", Moscow, 2009, p. 316.
[21] A.V. Malakhovskii, E.V. Eremin, D.A. Velikanov, A.V. Kartashev, A.D. Vasil'ev, I. A. Gudim, Fiz. Tverd. Tela 53 (2011) 1929 [Phys. Solid State 53 (2011) 2032].
[22] A.V. Malakhovskii, S.L. Gnatchenko, I.S. Kachur, V.G. Piryatinskaya, A.L. Sukhachev, V.L. Temerov, JMMM 375 (2015) 153.
[23] A.V. Malakhovskii, A.L. Sukhachev, A.A. Leont'ev, I.A. Gudim, A.S. Krylov, A.S. Aleksandrovsky, J. Alloys Compd. 529 (2012) 38.
[24] A.D. Balaev, L.N. Bezmaternykh, I.A. Gudim, V.L. Temerov, S.G. Ovchinnikov, S. A. Kharlamova, J. Magn. Magn. Mater. 258–259 (2003) 532.
[25] M.A. El'yashevitch. Spectra of Rare Earths, Moskow, 1953 (in Russian).
[26] A.V. Malakhovskii, S.L. Gnatchenko, I.S. Kachur, V.G. Piryatinskaya, A.L. Sukhachev, V.L. Temerov, J. Magn. Magn. Mater. 401 (2016) 517.
[27] A.V. Malakhovskii, A.L. Sukhachev, A.Yu. Strokova, I.A. Gudim, Phys. Rev. B 88 (2013) 075103.
[28] M.N. Popova, E.P. Chukalina, T.N. Stanislavchuk, B.Z. Malkin, A.R. Zakirov, E. Antic-Fidancev, E.A. Popova, L.N. Bezmaternykh, V.L. Temerov, Phys. Rev. B 75 (2007) 224435.
[29] A.V. Malakhovskii, A.L. Sukhachev, V.V. Sokolov, T.V. Kutsak, V.S. Bondarev, I.A. Gudim, J. Magn. Magn. Mater. 384 (2015) 255.
[30] D.V. Volkov, E.A. Popova, N.P. Kolmakova, A.A. Demidov, N. Tristan, Yu. Skourski, B. Buechner, I.A. Gudim, L.N. Bezmaternykh, JMMM 316 (2007) e717.
[31] V.V. Eremenko, N.E. Kaner, Yu.G. Litvinenko, V.V. Shapiro, Sov. Phys. JETP 57 (1983) 1312.